Research Paper

Cracking Characteristics of Different Crack Forms in Pavement under Moving Load

Guannan YAN

China Nuclear Power Engineering Co., Ltd.
Beijing 100840, China; e-mail: chyanguannan@126.com

In road engineering, the crack damage problems are one of the essential research areas that need to be emphasized. However, there have been few researches on the effects caused by different crack forms, e.g., the impacts of the distribution and propagation directions of formed cracks on subsequent cracking characteristics. In this study, two road models, including double cracks with different distribution and propagation directions, were established in ABAQUS software, and the potential cracking characteristics of such crack forms under moving load were investigated through numerical analysis. The simulation results demonstrated that the distribution and propagation directions of cracks are critical in affecting potential cracking modes and stress intensity factors. In more detail, a deeper crack tip with respect to the road surface tends to bring about the cracking with the first mode within a certain depth range. Additionally, a larger angle between the distribution direction of cracks and the traffic direction can promote the cracking with the second mode. Due to the too low numerical level of the stress intensity factor under the third mode at the middle crack tip, cracking with the third mode is generally unlikely for the middle zone of cracks in the pavement under a moving load. In view of this, on the premise that all cracks have the same sizes, a reflective crack is more likely to extend with the first mode than a top-down crack within a certain depth range, and compared with a longitudinal crack, a transverse crack has a higher potential to propagate with the second mode. Therefore, transverse reflective crack is a severe form of damage that needs to be detected as early as possible and repaired promptly.

Keywords: numerical analysis; cracking characteristics; different crack forms; stress intensity factors; transverse reflective crack.

1. Introduction

In road engineering, asphalt pavement structures are widely applied in many medium and high-grade highways. However, for asphalt pavements, crack damage is a common problem and significant investments are made annually to address it. Therefore, crack damage in asphalt pavement has become a point of interest for many experts and scholars in the field of road engineering.

Over the years, many types of laboratory tests have been utilized to investigate the cracking performance of asphalt concrete [1]. SAEIDI and AGHAYAN [2] conducted a semi-circular bending test to evaluate the cracking resistance of asphalt concrete samples in low-temperature environment, and the test results showed that aging can lead to a decrease in failure deformation, fracture energy and critical energy release rate, In addition, an increase in loading rate improves the peak load of samples but reduces failure deformation and fracture energy. FALCHETTO et al. [3] compared the low-temperature properties of asphalt mixtures obtained from the semi-circular bending test and the indirect tensile test, and a relationship between the two types of test results was established to predict the nominal strength under indirect tensile test based on partial results from the semi-circular bending test. BIRGISSON et al. [4] studied a three-point bending beam test to assess the cracking behaviors of asphalt mixtures. They found that tensile strength and fracture energy density can be used to characterize the cracking properties of both polymer-modified and unmodified asphalt mixtures, and the full-field strain maps showed that accumulated damage is distributed randomly in beam specimens, revealing that the accumulated damage is not only concentrated in the so-called fracture process zone (FPZ). On the basis of the three-point bending beam test, CHEN et al. [5] introduced a digital image correlation approach to describe cracking development in epoxy asphalt concrete samples. During their test, the digital image correlation approach was utilized to observe the three main stages of cracking: initiation, propagation and fracture failure. determined by the measured cracking sizes. Specific fracture parameters and the propagation route were further discussed based on these findings. In addition to the aforementioned tests, other tests such as the disk-shaped compact tension test [6], have been also used in relevant studies.

However, from a structural point of view, cracking behaviors of asphalt concrete specimens are different from those of asphalt pavement to some extent. Consequently, the results of laboratory tests cannot fully reflect the mechanical characteristics of actual asphalt pavement. In light of this, there is a need to conduct field measurements and establish a complete model of asphalt road in software. Compared to field measurements, the method of numerical analysis is undoubtedly more convenient and economical. With the development of computer technology, numerical analysis has gradually become an effective way to study the crack damage in asphalt pavement.

As early as 2006 and 2007, HUANG et al. [7, 8] applied the finite element method to simulate the stress intensity factors of cracked asphalt pavement, and they investigated the effects of vehicle speed and other influencing factors on stress intensity factors. With the help of numerical simulation, MIAO et al. [9] also analyzed the effects of vehicle speed, damping ratio and resilient modulus on the stress intensity factor under the first mode of the reflective crack in as-

phalt pavement. As another typical crack form in asphalt pavement, a top-down crack is also well worth investigating. ZHAO and TAN [10] pointed out that the cracking probability of the top-down crack in asphalt pavement on a semi-rigid base is lower than that on a granular base, and the ratio of the maximal stress intensity factors under the first mode and the second mode decreases when temperature and crack length increase. MIAO et al. [11] proposed a multi-domain hybrid boundary node method to simulate the stress intensity factors of top-down cracks, and the numerical examples proved that the presented method provides both high accuracy and fast convergence at the same time. AMERI et al. [12] calculated the stress intensity factors of top-down crack at different distances from the vehicle load, and the simulation results demonstrated that the signs and values of stress intensity factors are significantly dependent on the location relationship between the vehicle load and the crack plane. For rigid-flexible composite asphalt pavement, LI et al. [13] investigated its cracking and fatigue damage by combining fracture mechanics and damage mechanics. Recently, WANG and ZHONG [14] analyzed in detail the effects of tack coat on a reflective crack in asphalt pavement, and they found that the decrease of the modulus of the tack coat helps to prevent the growth of reflective crack.

Additionally, the discrete element method can be also utilized to simulate crack damage in asphalt pavement. CHE et al. [15] adopted the discrete element method to evaluate the cracking development in asphalt pavement under braking load. The simulation results showed that the initiation of micro-cracks is random and stochastic in asphalt pavement, and the propagation of micro-cracks exhibits discontinuous characteristics. The macro-fracture results from the thorough connection of enough local micro-cracks.

From the above studies, it can be observed that most scholars focused on the dynamic responses of pavement with a certain crack form, while few considered the cracking characteristics of cracks with different distribution and propagation directions. In the actual service environment, there exist inevitable differences among various crack forms, so the author of this paper pays attention to the service condition involving double cracks with different distribution and propagation directions in the pavement. On the other hand, in the above studies, the researchers employed several physical indices to evaluate the dynamic responses of cracked pavement under moving load. Among these indices, the stress intensity factor will be adopted in this study. Compared with other indices of stress, strain and displacement, the stress intensity factor can not only reflect dynamic responses but also reveal cracking characteristics by overcoming the singularity of the stress field near the crack tip. So in this study, with the help of ABAQUS software, two road models including double cracks are established, and the specific cracking characteristics of transverse top-down crack, longitudinal reflective crack, longitudinal top-down crack and transverse reflective crack were analyzed

using the evaluation index of the stress intensity factor. Through this study, it is hoped that the potential cracking modes of different crack forms in pavement under moving load can be further understood, providing beneficial guidance for future maintenance work.

2. Basic relevant principles

2.1. Principles in fracture mechanics

In fracture mechanics, practical phenomena of cracking and fracture can be abstracted as one or combination of following three modes, as shown in Fig. 1 [16]. According to the directions of external load and deformation, the first mode is called the open mode, the second mode is called the slide mode, and the third mode is known as the twist mode. The first mode is induced by tensile stress, so under this mode, cracks will open without any sliding deformations. At the current stage, cracking with the first mode is the most deeply studied because it is generally believed that the first mode causes the greatest harm to materials and structures in engineering. Both the second mode and the third mode are caused by shear stress. Hence, they both belong to the category of shear modes. The difference between them lies in that the second mode is one type of in-plane cracking, while the third mode is regarded as out-of-plane fracture.
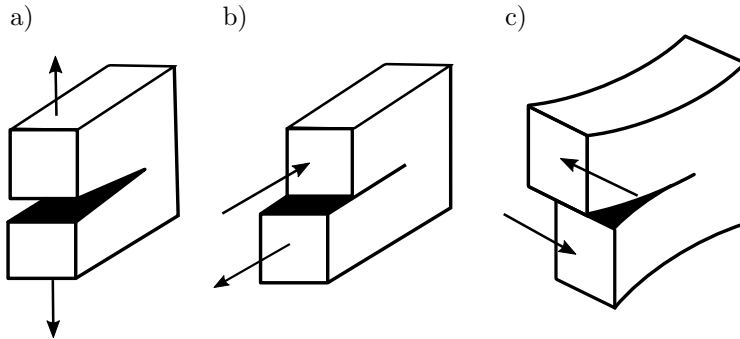

Fig. 1. Three typical fracture modes: a) open mode (the first mode); b) slide mode (the second mode); c) twist mode (the third mode).

It is known that the stress field near the crack tip has the singularity with $r^{-0.5}$ (r refers to the distance with respect to the crack tip), and to better describe the stress field with such singularity, the concept of stress intensity factor is introduced in fracture mechanics. According to the relationship among physical quantities, stress intensity factors can be expressed as formulas with stress vectors or formulas with displacement vectors. Since displacement vectors are

basic variables in the finite element method, the following simplified formulas are given:

$$(2.1) \qquad K_{\text{I}} \;=\; \frac{\sqrt{2\pi}E}{(1+\mu)\,(1+\chi)} \lim_{r\to 0} \frac{v(r)}{\sqrt{r}},$$

$$(2.2) \qquad K_{\text{II}} \;=\; \frac{\sqrt{2\pi}E}{(1+\mu)\,(1+\chi)} \lim_{r\to 0} \frac{u(r)}{\sqrt{r}},$$

$$(2.3) \qquad K_{\text{III}} \;=\; \frac{\sqrt{2\pi}E}{4\,(1+\mu)} \lim_{r\to 0} \frac{w(r)}{\sqrt{r}},$$

where K_{I}, K_{II} and K_{III} are the stress intensity factors under the first mode, the second mode and the third mode, respectively, $v(r)$ is the displacement vector perpendicular to the propagation direction of the crack, $u(r)$ is the displacement vector parallel to the propagation direction of the crack, $w(r)$ is the displacement vector perpendicular to the crack plane, r is the distance with respect to the crack tip, E is the elastic modulus, μ is Poisson's ratio; $\chi = (3 - \mu)/(1 + \mu)$ in plane stress condition, and $\chi = 3 - 4\mu$ in plane strain condition.

Limited by the length of this paper, the contents mentioned above serve only as a brief introduction, and more detailed information can be found in additional literature on fracture mechanics.

2.2. Principles in finite element method

In order to obtain the stress intensity factors of the cracks in asphalt pavement, the finite element method was adopted in this study. Specifically, the Dynamic/Implicit module in the ABAQUS software was employed to calculate the stress intensity factors of the cracks under vehicle load, and the governing motion equation can be expressed as:

$$(2.4) \qquad [M]\,\{a\} + [C]\,\{v\} + [K]\,\{d\} = \{F\},$$

where $[M]$, $[C]$ and $[K]$ are the mass matrix, damping matrix and stiffness matrix, respectively, $\{a\}$, $\{v\}$ and $\{d\}$ are acceleration vectors, vectors and displacement vectors, respectively (all the motion vectors involve three orthogonal directions), and $\{F\}$ represents the external resultant load.

Based on Eq. (2.4), the displacement field of the area around the crack tip can be determined, and then the three types of stress intensity factors can be further obtained by solving Eqs. (2.1)–(2.3).

3. Finite element models

3.1. Model prototype and material parameters

In this study, the prototype of finite element models is an actual road section that is located in Kunming City, Yunnan Province, China, as shown in Fig. 2. Material parameters used in this study were determined based on cored samples in the field and the results of compressive strength test and resilient modulus test, as shown in Table 1 [17]. It is important to point out that the material parameters were obtained at a temperature of 20°C, which is approximately the normal temperature in the field, and the road model can be characterized by the combination of two parts: elastomer and Rayleigh model [18, 19]. Resilient modulus, a key material parameter of the elastomer, was applied in this study. According to Appendix E in the Specifications for the Design of Highway Asphalt Pavement (JTG D50-2006) [20], the recommended resilient moduli of asphalt layers are usually within the numerical range of 1200–1600 MPa under 20°C. Since the actual road section is not a road section with very high grade, it can be considered that the magnitudes of resilient modulus test results, which are slightly less than the recommended lower limit value of 1200 MPa, are reasonable. Moreover, the Rayleigh model was utilized to reflect the absorption and attenuation of vibration energy due to the viscoelasticity of the asphalt pavement [21]: for asphalt layers, damping ratio $\zeta = 0.05$, mass damping coefficient $\alpha = 0.93$, and stiffness damping coefficient $\beta = 0.0027$; for the earth foundation, the damping ratio remains constant, $\alpha = 0.41$, and $\beta = 0.0061$.

Fig. 2. Actual road section.

Table 1. Basic material parameters of structural layers.

Structural layer	Main component	Thickness [cm]	Density [kg·m^{-3}]	Modulus [MPa]	Poisson's ratio
Top layer	AC-13	2	2300	1200	0.35
Bottom layer	AC-20	3	2250	1100	0.35
Base layer	Penetrated asphalt	5	2200	900	0.35
Subgrade	Soil	–	1800	50	0.40

3.2. Establishment of cracked road models

In the ABAQUS software, two road models including double cracks were established on the basis of an intact road model verified in the previous study [17], and the two road models were named Model 1 and Model 2 in this study. Except for the distribution and propagation directions of double cracks, the geometry dimensions, displacement constraints and applied external load of the two road models kept consistent with each other. The length, width and height of each road model were 7.50 m, 3.75 m, and 3.75 m, respectively. In terms of the displacement constraints, all the degrees of freedom at the bottom of each road model were restrained, and the degrees of freedom along the normal directions of the front, rear, left and right sides were also restrained. With respect to the applied external load, the amplitude of semi-sinusoidal load was set to 0.70 MPa that is the grounding pressure under the standard axle load of 100 kN in China, and the tire-ground contact shape was simplified as five closely connected rectangles, as shown in Fig. 3 [22, 23]. Additionally, the DLOAD subroutine was employed to simulate a single tire passing by the cracked area at 36 km/h, and the loading time was set to 0.18 s accordingly.
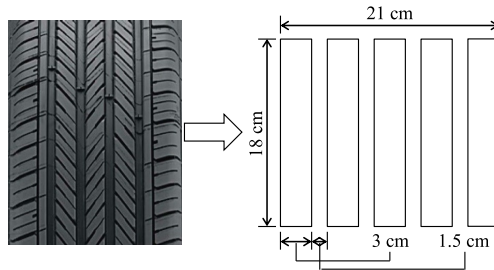

FIG. 3. Simplified tire-ground contact shape.

On the other hand, the difference between the two road models was the distribution and propagation directions of double cracks, as summarized in Table 2. In Model 1, one crack perpendicular to the traffic direction was set as a top-down crack in top layer, and the other crack parallel to the moving direction of the vehicle load was set as a reflective crack in the base layer. Meanwhile, the locations of the double cracks in Model 2 were swapped, suggesting that the

Table 2. Preset cracks in Model 1 and Model 2.

Road model	Transverse top-down crack	Longitudinal reflective crack	Longitudinal top-down crack	Transverse reflective crack
Model 1	In the top layer	In the base layer	–	–
Model 2	–	–	In the top layer	In the base layer

transverse crack was moved down to the base layer to represent a reflective crack, and the longitudinal crack was moved up to the top layer to make it a top-down crack. For the four preset cracks, the lengths along the distribution and propagation directions were 42 cm and 1 cm, and the buried depths of the crack tips of the top-down crack and reflective crack were 1 cm and 7 cm. In addition, all the cracks were set within the central area of asphalt pavement where the single
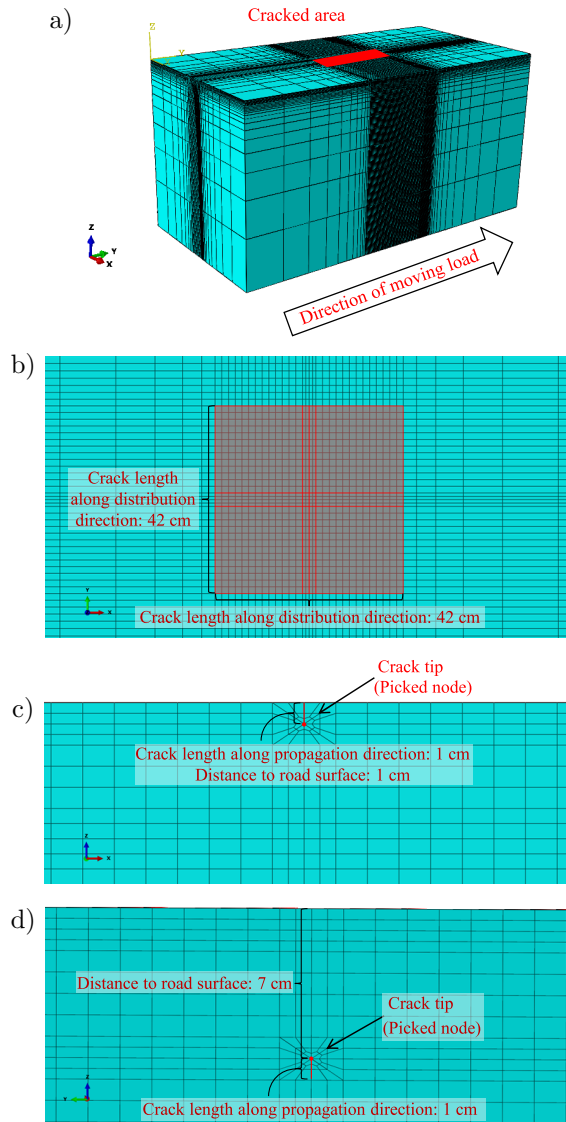

FIG. 4. Meshed cracked road model: a) overall view of road model; b) enlarged top view of transverse crack and longitudinal crack; c) enlarged side view of top-down crack; d) enlarged side view of reflective crack.

tire load was applied. After meshing, each road model contained 165 408 mesh elements whose type is 8-node linear brick with reduced integration (C3D8R), and the refined meshes were used in the cracked area, as shown in Fig. 4.

4. Results and discussions

According to fracture mechanics, the positive stress intensity factor under the first mode can induce the development of open cracks, while the stress intensity factor with a negative value under the first mode does not have any inciting effects on the extension of open cracks, and such a stress intensity factor can only characterize the singularity of the stress field near the crack tip. For the stress intensity factors under the second mode and the third mode, regardless of whether their numerical values are positive or negative, nonzero values will incite the shear propagation of cracks.

Generally, it is difficult to directly calculate the stress intensity factors of cracks using the Dynamic/Explicit module in ABAQUS software, so the stress intensity factors at and near the crack tip can be obtained only by the method of extrapolation. In comparison, the Dynamic/Implicit module can calculate and output stress intensity factors automatically within every iteration, and the simulation results from this module have relatively high accuracy and reliability.

4.1. Simulation results in Model 1

Figures 5 and 6 illustrate the time-history curves of the stress intensity factors of the cracks in Model 1. The selected nodes for the calculation of the stress intensity factors in the following figures are located at the respective middle crack tips of the transverse top-down crack and the longitudinal reflective crack. In other words, the two nodes are on the central vertical line of each road model and they are 1 cm and 7 cm away from road surface. In addition, for better subsequent comparison, the units of all the three types of stress intensity factors have been unified as $\mathrm{Pa} \cdot \mathrm{m}^{0.5}$.

It can be seen from Fig. 5 that there are sign changes for the three types of stress intensity factors of the transverse top-down crack. During the overall loading period, it is found that the stress intensity factor under the first mode of the transverse top-down crack changes from positive to negative with the approach of tire, and changes from negative to positive as the tire leaves, indicating that the vehicle load tends to close the transverse top-down crack rather than open it. For the stress intensity factor under the second mode of the transverse top-down crack, its sign also changes when the tire passes by, and its numerical value keeps nonzero state in almost whole loading period, which means that transverse top-down crack is very likely to develop with the second mode.
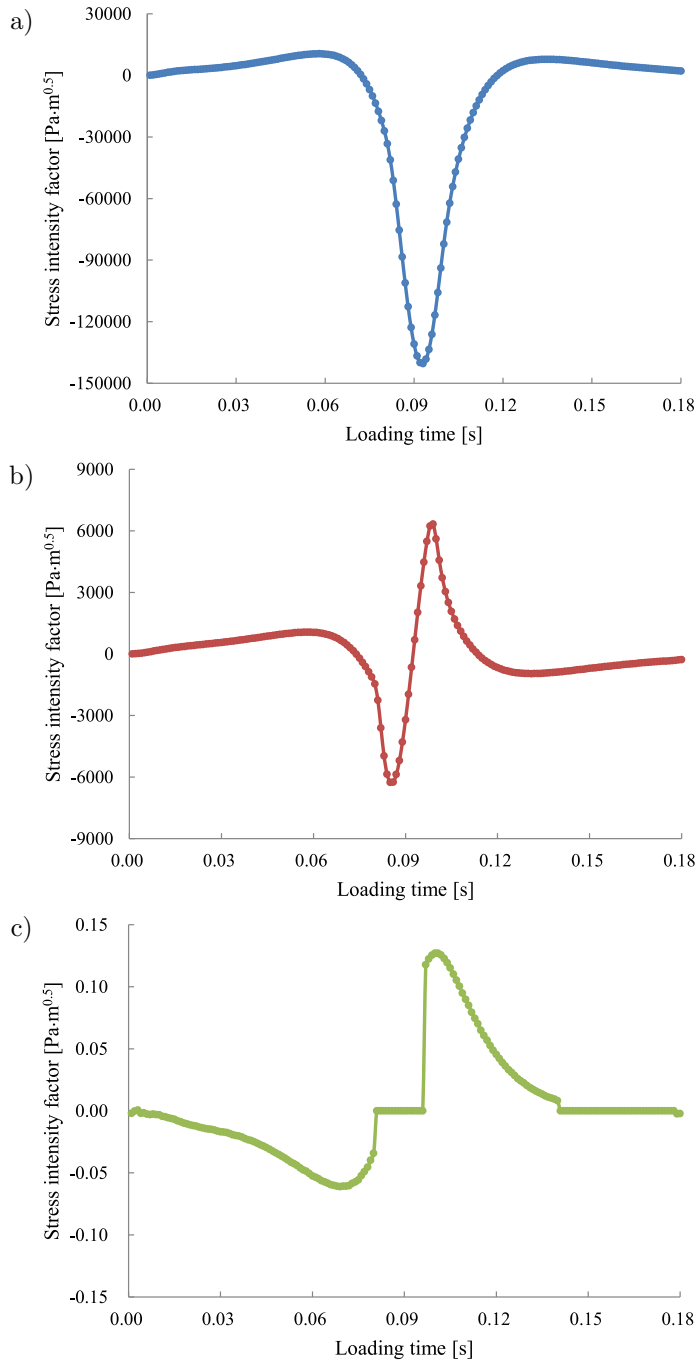
FIG. 5. Stress intensity factors of transverse top-down crack: a) stress intensity factor under the first mode; b) stress intensity factor under the second mode; c) stress intensity factor under the third mode.
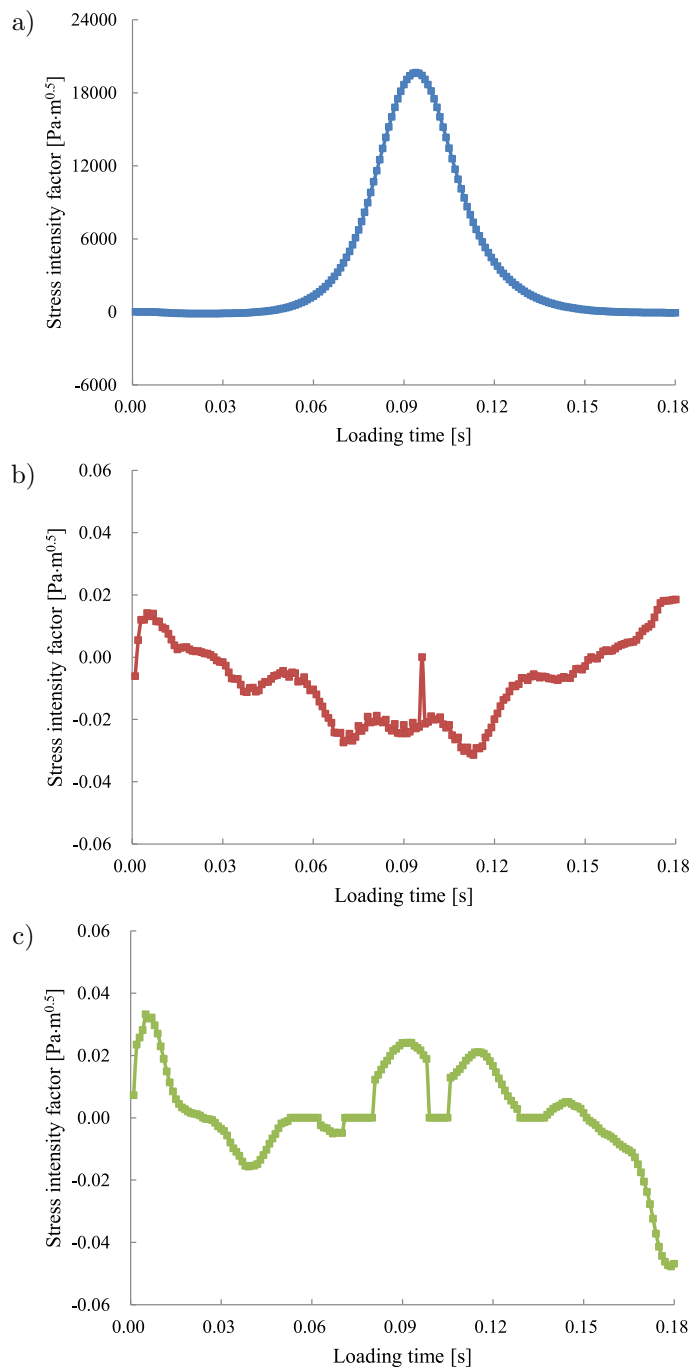
FIG. 6. Stress intensity factors of longitudinal reflective crack: a) stress intensity factor under the first mode; b) stress intensity factor under the second mode; c) stress intensity factor under the third mode.

Compared with the above two types of stress intensity factors, the stress intensity factor under the third mode at the middle crack tip can be ignored, in other words, the middle zone of transverse top-down crack is unlikely to extend with the third mode. Based on the curve trends of the stress intensity factors under three modes, it is believed that the transverse top-down crack in the asphalt pavement has a great potential for cracking with the mode of in-plane shear under vehicle load.

In Fig. 6, the stress intensity factor under the first mode always remains positive within entire loading period, indicating that the longitudinal reflective crack tends to propagate upward with the first mode. Moreover, there is a significant difference in the order of the magnitude of the stress intensity factors between the open mode and the two types of shear modes, so the stress intensity factors under the second mode and the third mode can be neglected for the longitudinal reflective crack. Hence, the longitudinal reflective crack in Model 1 is most likely to develop with the open mode instead of any shear modes.

4.2. Simulation results in Model 2

As shown in Figs. 7 and 8, the stress intensity factor data at the respective middle crack tips of the cracks in Model 2 were also extracted and plotted. It can be observed from Fig. 7 that the stress intensity factor under the first mode of the longitudinal top-down crack is negative, and the stress intensity factors under other two modes are so close to zero that can be ignored. This reveals that when the distribution direction of the top-down crack is parallel to the traffic direction, the vehicle load will not incite the downward development of the longitudinal top-down crack directly. In this case, the continuous growth of such a crack form is more a result of the performance degradation of pavement materials during the service life, which is closely related to environmental factors.

Similarly, the potential cracking characteristics of the transverse reflective crack can be also evaluated according to the signs and values of the stress intensity factors under three modes. The time-history curve in Fig. 8a shows that when the vehicle load arrives, the stress intensity factor under the first mode becomes positive, so the cracking with the first mode may occur in the transverse reflective crack. Meanwhile, Fig. 8b reflects that the approaching vehicle load makes the stress intensity factor under the second mode reach a relatively high numerical level. From Fig. 8c, it can be concluded that there is no possibility of cracking with the twist mode for the middle zone of the transverse reflective crack because the magnitude of the stress intensity factor under the third mode at the middle crack tip is negligible. Therefore, the transverse reflective crack in Model 2 has the potential to extend with both the first mode and the second mode at the same time.
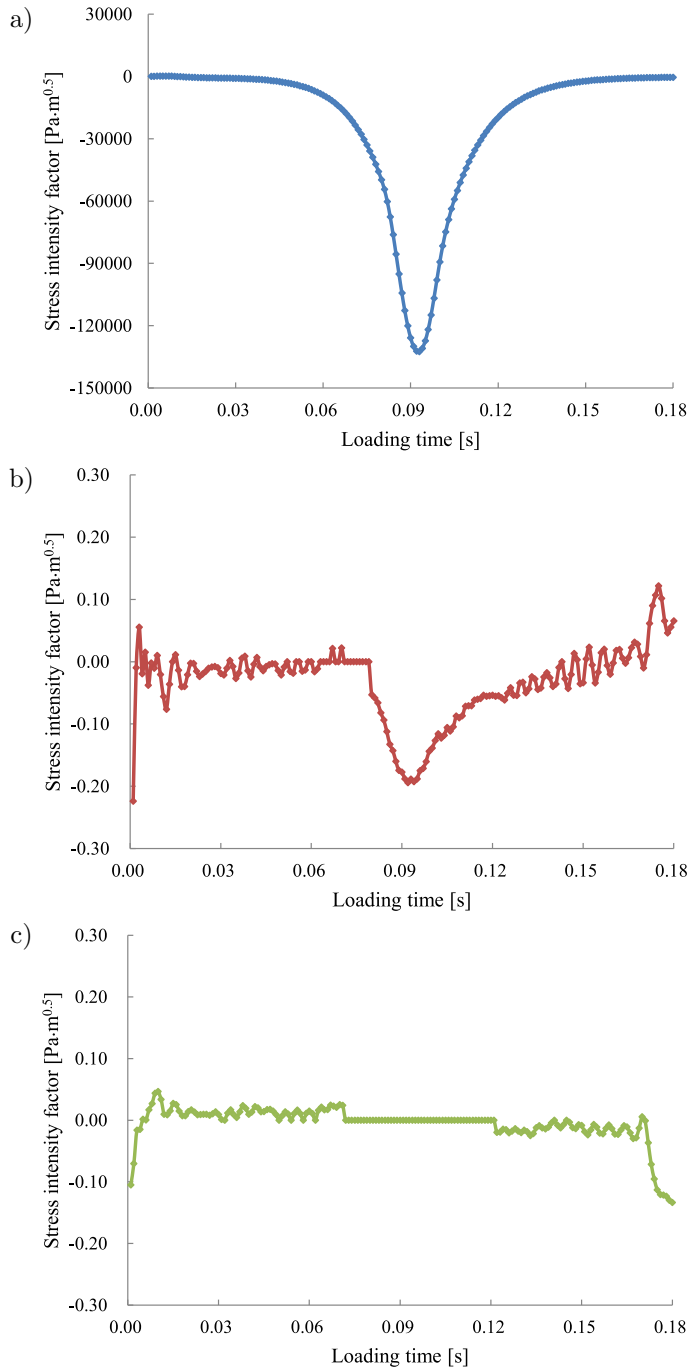
FIG. 7. Stress intensity factors of longitudinal top-down crack: a) stress intensity factor under the first mode; b) stress intensity factor under the second mode; c) stress intensity factor under the third mode.
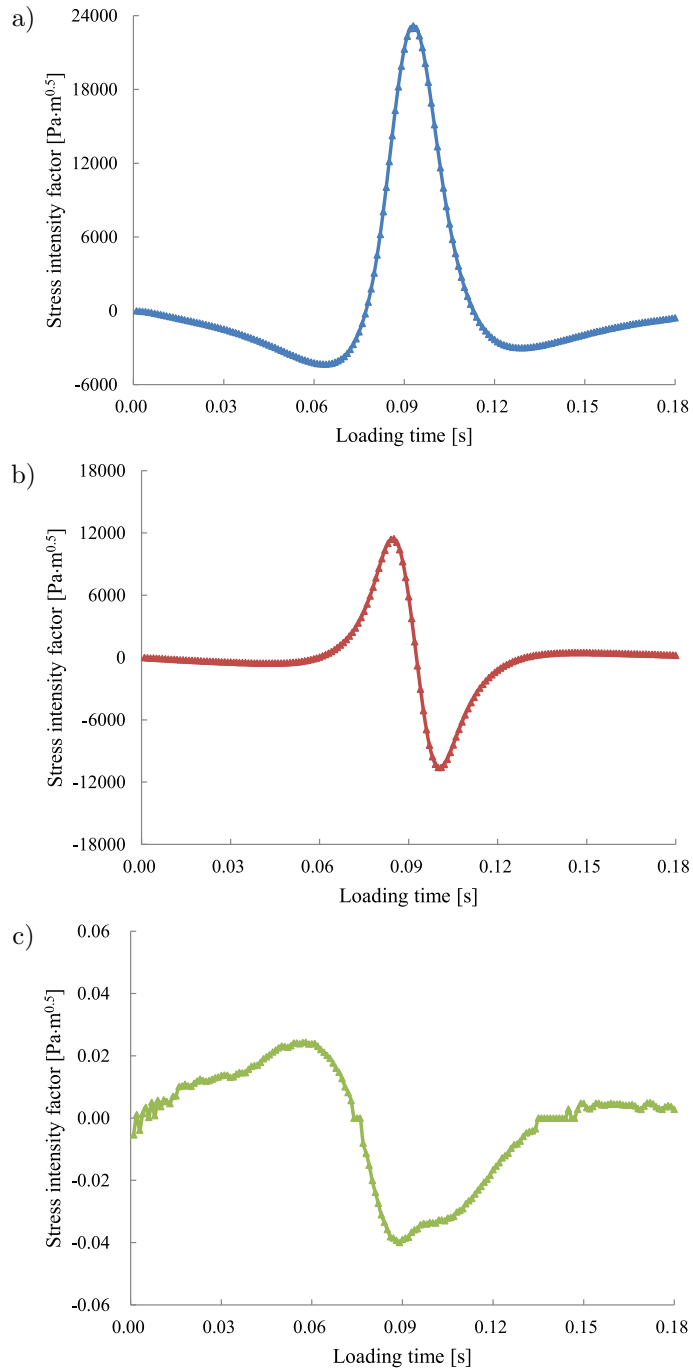
FIG. 8. Stress intensity factors of transverse reflective crack: a) stress intensity factor under the first mode; b) stress intensity factor under the second mode; c) stress intensity factor under the third mode.

4.3. Relevant discussion

According to Figs. 5–8, from the numerical level, the stress intensity factor under the first mode has the highest absolute value, which suggests that once the stress intensity factor under the first mode is positive, there will be the maximal possibility of the cracking with open mode in asphalt pavement. In terms of the stress intensity factor under the second mode, its numerical value varies significantly for different crack forms. For the transverse top-down crack and transverse reflective crack, their stress intensity factors under the second mode vary within a wide numerical range, while for the longitudinal top-down crack and longitudinal reflective crack, the numerical values of such stress intensity factors can be considered as zero. As for the stress intensity factor under the third mode, its numerical value at the middle crack tip is negligible regardless of the distribution or propagation direction of cracks, meaning that out-of-plane cracking is hard to occur for the middle zone of cracks in asphalt pavement under vehicle load.

It can be further observed that when the vehicle load moves directly just above the cracks in asphalt pavement, the stress intensity factor under the first mode of the top-down crack is negative, while that of the reflective crack is positive. This is related to the buried depth of the crack tip and the distribution of tensile stress and compressive stress. Specifically, tensile stress dominates the first mode of cracking, but the pressure from vehicles leads to significant compressive stress near the road surface. With the increase of depth, both tensile stress and compressive stress decrease in general. According to the simulation results, compressive stress decreases rapidly with distance from the vehicle load, and the decrease rate of compressive stress is faster than that of tensile stress. In view of this, the stress intensity factor under the first mode changes from negative to positive gradually as the depth increases, indicating that the crack with a deeper crack tip is more likely to propagate with the first mode within a certain depth range. Of course, although the stress intensity factor under the first mode of reflective crack is positive, its absolute value is still much lower than that of the top-down crack due to the repression effect of depth on stress intensity factors. Overall, compared with the top-down crack, the reflective crack continues to develop easier. In Model 1, the maximal stress intensity factor of the longitudinal reflective crack is $19\,666\,\mathrm{Pa}\cdot\mathrm{m}^{0.5}$ (corresponding to the stress intensity factor under the first mode); for the transverse top-down crack, the stress intensity factor under the second mode is dominant, and its maximum is $6332\,\mathrm{Pa}\cdot\mathrm{m}^{0.5}$. In Model 2, open mode and slide mode are both available for the transverse reflective crack, and the peak value of the stress intensity factor under the first mode is up to $23\,175\,\mathrm{Pa}\cdot\mathrm{m}^{0.5}$; while the effective peak of the stress intensity factors of the longitudinal top-down crack is less than $0.30\,\mathrm{Pa}\cdot\mathrm{m}^{0.5}$

(the extremum of the stress intensity factor under the second mode is only about $-0.20\,\mathrm{Pa\cdot m^{0.5}}$).

On the other hand, in addition to vertical stress, the vehicle load produces horizontal stress at the same time, so the cracking with the second mode related to plane shear stress may also exist in asphalt pavement. If the distribution direction of cracks is perpendicular to the traffic direction, such a crack form will be fully subjected to the horizontal impact and shear stress caused by vehicles, and the probability of the cracking with slide mode will rise accordingly, which reflects that the larger angle between the distribution direction of cracks and the traffic direction helps to promote the cracking with the second mode. From this perspective, the potential influences of transverse cracks on asphalt pavement are greater than those of longitudinal cracks. If top-down crack is taken as an example, the transverse top-down crack in Model 1 has a tendency fir extension with the second mode, but the longitudinal top-down crack in Model 2 is not sensitive to vehicle load; if the reflective crack is taken as another example, the longitudinal reflective crack in Model 1 possibly can propagate with the first mode, and for the transverse reflective crack in Model 2, there is cracking with a mixed mode consisting of the first mode and the second mode. Therefore, it can be seen that the angle between the distribution direction of cracks and the traffic direction is a critical factor greatly affecting the development of the cracks in asphalt pavement. Furthermore, both the time-history curves of the stress intensity factors under the second mode of the transverse top-down crack and the transverse reflective crack present anti-symmetry around the middle time of the whole loading period, and that is because the direction of the horizontal shear stress acting on the transverse cracks changes by nearly $180°$ at that moment. Besides, the waveforms of the two corresponding curves also display anti-symmetry to each other, revealing that the direction of the horizontal shear stress acting on the two cracks is opposite to each other.

5. Conclusions

In this study, to better master the potential cracking characteristics of cracks with different distribution and propagation directions in pavement under moving load, two cracked road models were established in the finite element software ABAQUS, and each road model had double cracks, i.e., the transverse top-down crack and longitudinal reflective crack in Model 1, and the longitudinal top-down crack and transverse reflective crack in Model 2. Based on the investigation on the stress intensity factors of the four preset cracks, the main conclusions can be drawn as follows.

(1) The magnitude of the stress intensity factor under the first mode is the largest, and whether the cracks in pavement continue growing depends

on the sign of the stress intensity factor under the first mode. The stress intensity factor under the third mode at the middle crack tip is too small to have effects on the growth of the middle zone of cracks, while the numerical value of the stress intensity factor under the second mode varies greatly according to different crack forms.

(2) The buried depth of the crack tip is significant for the stress intensity factor under the first mode, and within a certain depth range, the cracking with the first mode is more likely to occur in the crack with a deeper crack tip. The angle between the distribution direction of cracks and the traffic direction is critical to the stress intensity factor under the second mode, and the cracking with the second mode usually exists in the crack with a larger such angle.

(3) The potential cracking characteristics of cracks are closely related to crack forms, and specific cracking modes largely depend on the distribution and propagation directions of the cracks in pavement. Compared with the top-down crack and longitudinal crack, the reflective crack and transverse crack with the same sizes have higher potential to continue extending, so transverse reflective crack is a severe damage form that needs to be paid sufficient attention to in practical road engineering.

The above conclusions help to explain which cracking mode the formed cracks are the most likely to continue developing with and provide an insight into the roles and effects of the distribution and propagation directions of formed cracks.

In future studies, although the prototype model in this study has been validated previously, it is necessary to try to obtain the relevant field measurement data to further confirm the numerical analysis results on the stress intensity factors of such two cracked road models. Due to the difficulty in direct confirmation, smart aggregate technology may be utilized to monitor the growth rates of different crack forms in pavement, so as to verify the simulation results formed in this study from the side. Besides, the effects brought by temperature field, horizontal force, multiple cracks' interaction and the location relationship between tire and crack should be further considered to conduct a more comprehensive numerical analysis at the next stage.

References

1. AL-QUDSI A., FALCHETTO A.C., WANG D., BÜCHLER S., KIM Y.S., WISTUBA M.P., Finite element cohesive fracture modeling of asphalt mixture based on the semi-circular bending (SCB) test and self-affine fractal cracks at low temperatures, *Cold Regions Science and Technology*, **169**: 102916, 2020, doi: 10.1016/j.coldregions.2019.102916.

2. SAEIDI H., AGHAYAN I., Investigating the effects of aging and loading rate on low-temperature cracking resistance of core-based asphalt samples using semi-circular bending

test, *Construction and Building Materials*, **126**: 682–690, 2016, doi: 10.1016/j.conbuild mat.2016.09.054.

3. FALCHETTO A.C., MOON K.H., WANG D., RICCARDI C., WISTUBA M.P., Comparison of low-temperature fracture and strength properties of asphalt mixture obtained from IDT and SCB under different testing configurations, *Road Materials and Pavement Design*, **19**(3): 591–604, 2018, doi: 10.1080/14680629.2018.1418722.

4. BIRGISSON B., MONTEPARA A., ROMEO E., TEBALDI G., Characterisation of asphalt mixture cracking behaviour using the three-point bending beam test, *International Journal of Pavement Engineering*, **12**(6): 569–578, 2011, doi: 10.1080/10298436.2011.565766.

5. CHEN L.L., QIAN Z.D., LU Q., Crack initiation and propagation in epoxy asphalt concrete in the three-point bending test, *Road Materials and Pavement Design*, **15**(3): 507–520, 2014, doi: 10.1080/14680629.2014.908132.

6. CHIANGMAI C.N., BUTTLAR W.G., Cyclic loading behavior of asphalt concrete mixture using disk-shaped compact tension (DC(T)) test and released energy approach, *Asphalt Paving Technology: Association of Asphalt Paving Technologists – Proceedings of the Technical Sessions*, **84**: 593–614, 2015.

7. HUANG Z.Y., WANG J.C., ZHU X.R., Viscoelastic fracture analysis of asphalt concrete pavement with cracks, *China Journal of Highway and Transport* [in Chinese], **19**(2): 18–23, 2006.

8. HUANG Z.Y., WANG J.C., ZHU X.R., Viscoelastic analysis of asphalt pavement with reflective cracks and subjected to dynamic loading, *Journal of Zhejiang University (Engineering Science Edition)* [in Chinese], **41**(1): 114–119, 2007.

9. MIAO Y., WAN Y.D., ZHANG S.M., Dynamic response analysis of asphalt pavement with reflective crack, *Rock and Soil Mechanics* [in Chinese], **30**(8): 2511–2516, 2009.

10. ZHAO Y.Q., TAN Y.Q., Analysis of top-down cracking of asphalt pavements based on fracture mechanics approach, *Journal of Tongji University (Natural Science Edition)* [in Chinese], **38**(2): 218–222, 2010.

11. MIAO Y., HE T.G., YANG Q., ZHENG J.J., Multi-domain hybrid boundary node method for evaluating top-down crack in asphalt pavements, *Engineering Analysis with Boundary Elements*, **34**(9): 755–760, 2010, doi: 10.1016/j.enganabound.2010.04.002.

12. AMERI M., MANSOURIAN A., HEIDARY KHAVAS M., ALIHA M.R.M., AYATOLLAHI M.R., Cracked asphalt pavement under traffic loading – A 3D finite element analysis, *Engineering Fracture Mechanics*, **78**(8): 1817–1826, 2011, doi: 10.1016/j.engfracmech.2010.12.013.

13. LI S., LI Y.Z., LIU Z.H., Research on temperature fatigue damage and cracking in asphalt layer of rigid-flexible composite pavement, *Engineering Mechanics* [in Chinese], **30**(10): 122–127, 2013, doi: 10.6052/j.issn.1000-4750.2012.06.0448.

14. WANG X.Y., ZHONG Y., Influence of tack coat on reflective cracking propagation in semi-rigid base asphalt pavement, *Engineering Fracture Mechanics*, **213**: 172–181, 2019, doi: 10.1016/j.engfracmech.2019.04.015.

15. CHE F., CHEN S.F., LI Z.H., LIU W.D., WANG A.X., Analysis of cracks propagation on asphalt pavement surface under load, *Journal of Highway and Transportation Research and Development* [in Chinese], **27**(5): 26–29, 2010, doi: 10.1214/10-AAP750.

16. XIE D., QIAN Q., LI C.A., *Numerical Methods and Engineering Application in Fracture Mechanics* [in Chinese], Science Press, Beijing, China, 2009.

17. YAN G.N., YE Z.J., WANG W.T., WANG L.B., Numerical analysis on distribution and response of acceleration field of pavement under moving load, *International Journal of Pavement Research and Technology*, **14**(5): 519–529, 2021, doi: 10.1007/s42947-020-0179-9.

18. YANG H.L., ZHAO Q., GUO X.L., ZHANG W.D., LIU P.F., Wang L.B., Numerical analysis of signal response characteristic of piezoelectric energy harvesters embedded in pavement, *Materials*, **13**(12): 2770, 2020, doi: 10.3390/ma13122770.

19. YE Z.J., MIAO Y.H., ZHANG W.D., WANG L.B., Effects of random non-uniform load on asphalt pavement dynamic response, *International Journal of Pavement Research and Technology*, **14**(3): 299–308, 2021, doi: 10.1007/s42947-020-0147-0.

20. Ministry of Transport of the People's Republic of China, *Specifications for Design of Highway Asphalt Pavement (JTG D50-2006)* [in Chinese], China Communications Press, Beijing, China, 2006.

21. LIAO G.Y., HUANG X.M., *Application of ABAQUS Finite Element Software in Road Engineering* [in Chinese], Southeast University Press, Nanjing, China, 2008.

22. DONG Z.J., TAN Y.Q., OU J.P., Dynamic response analysis of asphalt pavement under three-directional nonuniform moving load, *China Civil Engineering Journal* [in Chinese], **46**(6): 122–130, 2013, doi: 10.15951/j.tmgcxb.2013.06.003.

23. YE Z.J., LU Y., WANG L.B., Investigating the pavement vibration response for roadway service condition evaluation, *Advances in Civil Engineering*, **2018**: 2714657, 2018, doi: 10.1155/2018/2714657.